

Supporting Information

A cytotoxic BODIPY-appended half-sandwich iridium(III) complex forms protein adducts and induces ER stress

Robin Ramos,^{††} Jean-François Gilles,[#] Romain Morichon,[‡] Cédric Przybylski[†], Benoît Caron,[§] Candice Botuha,[†] Anthi Karaiskou,[‡] Michèle Salmain^{*†} and Joëlle Sobczak-Thépot^{*‡}

[†] Institut Parisien de Chimie Moléculaire (IPCM), Sorbonne Université, CNRS, 4 place Jussieu, F-75005 Paris, France.

*E-mail: michele.salmain@sorbonne-universite.fr

[‡] Centre de Recherche Saint Antoine (CRSA), Sorbonne Université, INSERM, 184 rue du Faubourg Saint Antoine, F-75012 Paris, France.

* E-mail: joelle.sobczak@inserm.fr

[#] Imaging Core Facility, CNRS-FR3631-Institut de Biologie Paris Seine, Sorbonne Université, F-75005, Paris, France

[§] Sorbonne Université, ISTeP, ALIPP6, 4 place Jussieu 75005 Paris

Supplementary figures

Figure S1 – Synthetic pathway to IrBDP and IrBDP⁺ and atom numbering	S2
Figure S2 – Stability and ligand exchange of IrBDP in DMSO- <i>d</i> ₆	S3
Figure S3 – Spectral properties of IrBDP and IrBDP⁺	S4
Figure S4 – Inhibition of hTERT-RPE1 cells proliferation upon IrBDP treatment	S5
Figure S5 – Internalization and fluorescence spectra of IrBDP in cells	S6
Figure S6 – Internalization of IrBDP and phox-BDP	S7
Figure S7 – IrBDP is not internalized by endocytosis.....	S8
Figure S8 – IrBDP accumulates in the mitochondria.....	S9
Figure S9 – IrBDP stains a small proportion of lysosomes	S10
Figure S10 – Characterization of cytoplasmic vacuoles formed upon IrBDP treatment	S11
Figure S11 – ER-stress markers in response to IrBDP treatment.....	S12
Figure S12 – Kinetics of the activation of ER-stress markers analyzed by Western Blot	S13
Figure S13 – IrBDP forms covalent adducts with proteins <i>in vitro</i>	S14

Supplementary tables

Table S1 – Observed adducts (HR-MS) ; relative intensity of peaks	S15
Table S2 – Photophysical parameters of IrBDP , IrBDP⁺ and phox-BDP in various solvents .	S15

Supplementary videos links

1. Addition of neutral IrBDP into DMSO	S15
2. Sample videomicroscopy: 8 μM phox-BDP treatment of HeLa cells	S15
3. Sample videomicroscopy: 8 μM IrBDP treatment of HeLa cells	S15
4. Cell fluorescence after IrBDP treatment	S15

Annexes

Annex 1. ¹ H and ¹³ C NMR spectra of IrBDP	S16
Annex 2. ¹ H and ¹³ C NMR spectrum of phox-BDP	S17
Annex 3. HRMS spectra of IrBDP incubated with two substrates	S18
Annex 4. RP-HPLC chromatograms of phox-BDP and IrBDP	S20

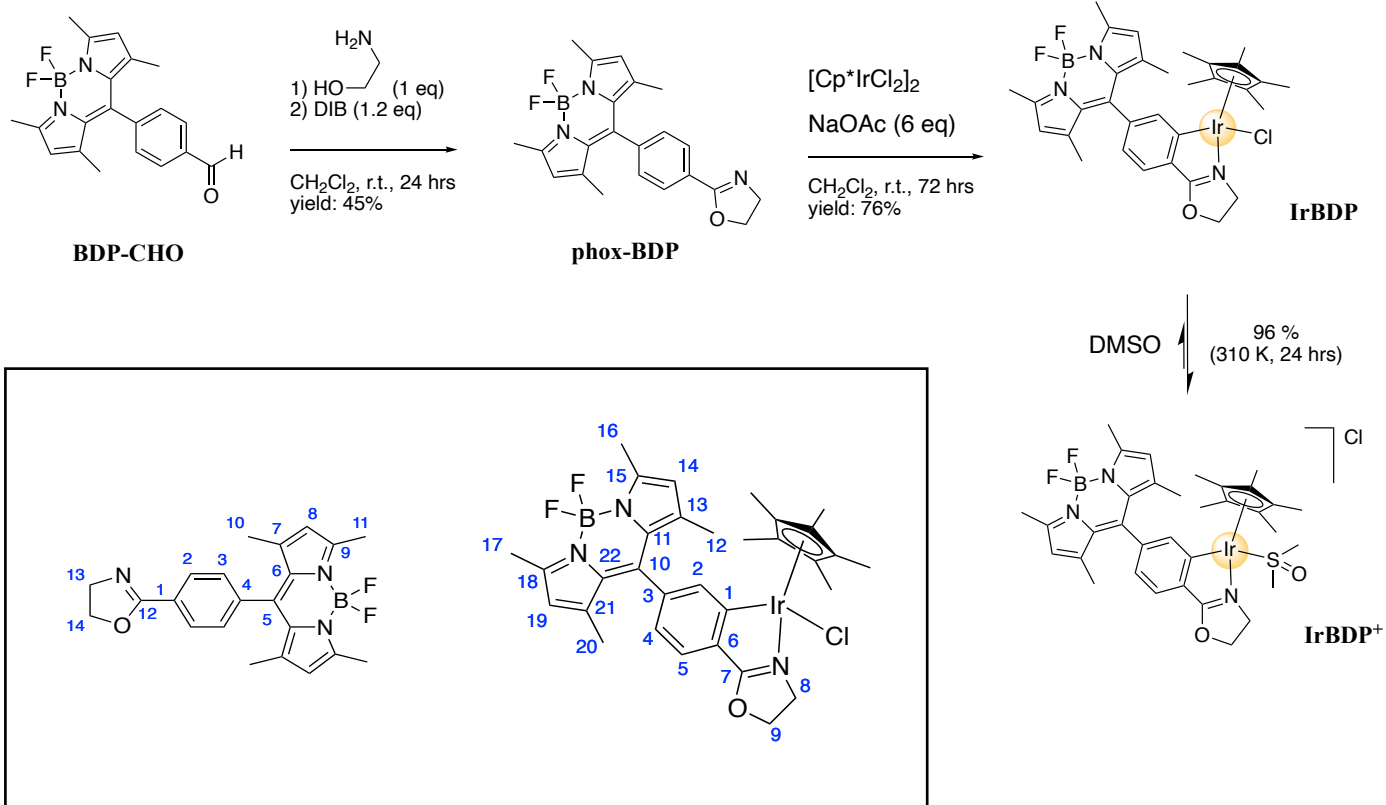
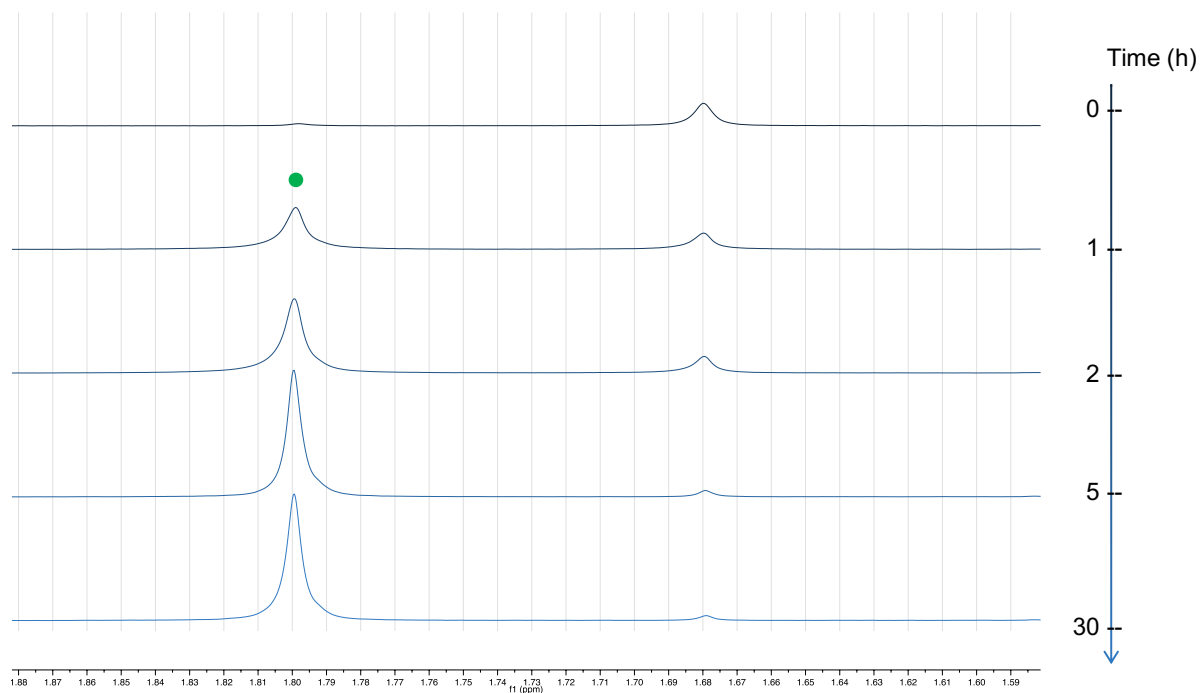


Figure S1 – Synthetic pathway to IrBDP and IrBDP⁺ and atom numbering

a.



b.

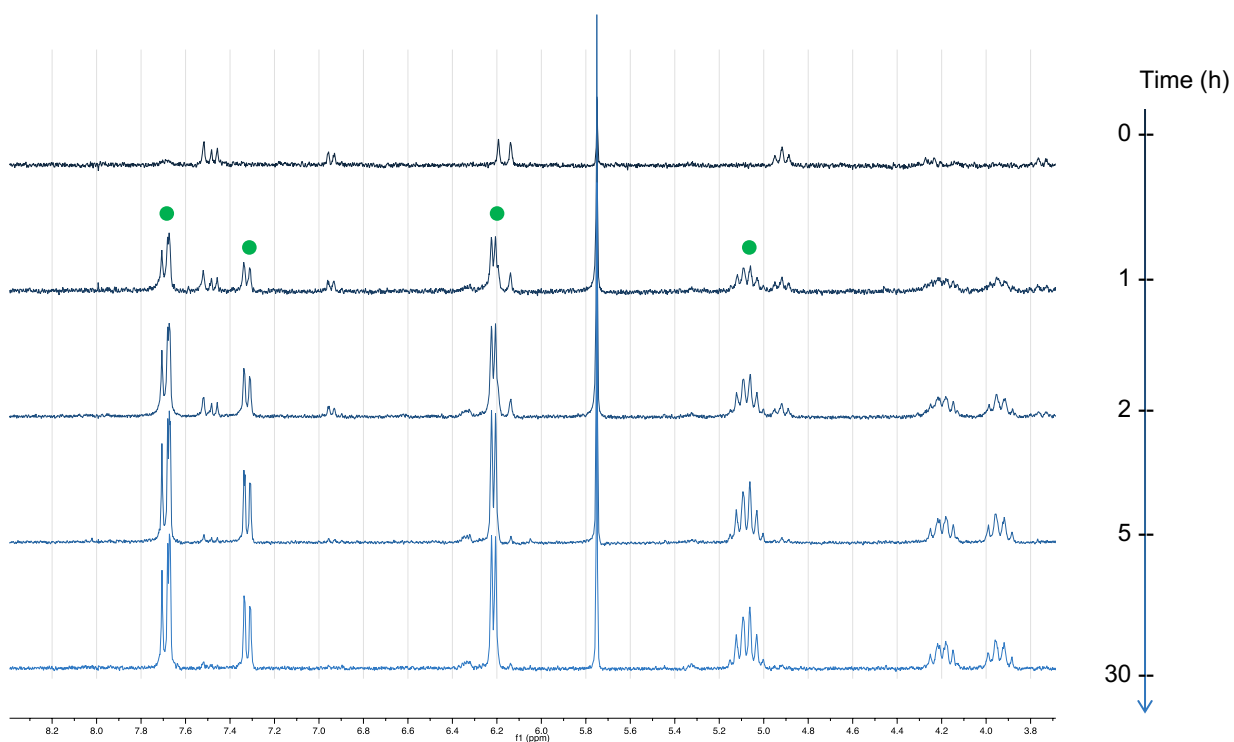


Figure S2 – Stability and ligand exchange of **IrBDP** in DMSO-d₆
¹H NMR spectra of **IrBDP** in DMSO-d₆ between 0 and 30 h (dark blue to light blue)

a. Cp* region

b. Aromatic region

● : IrBDP⁺

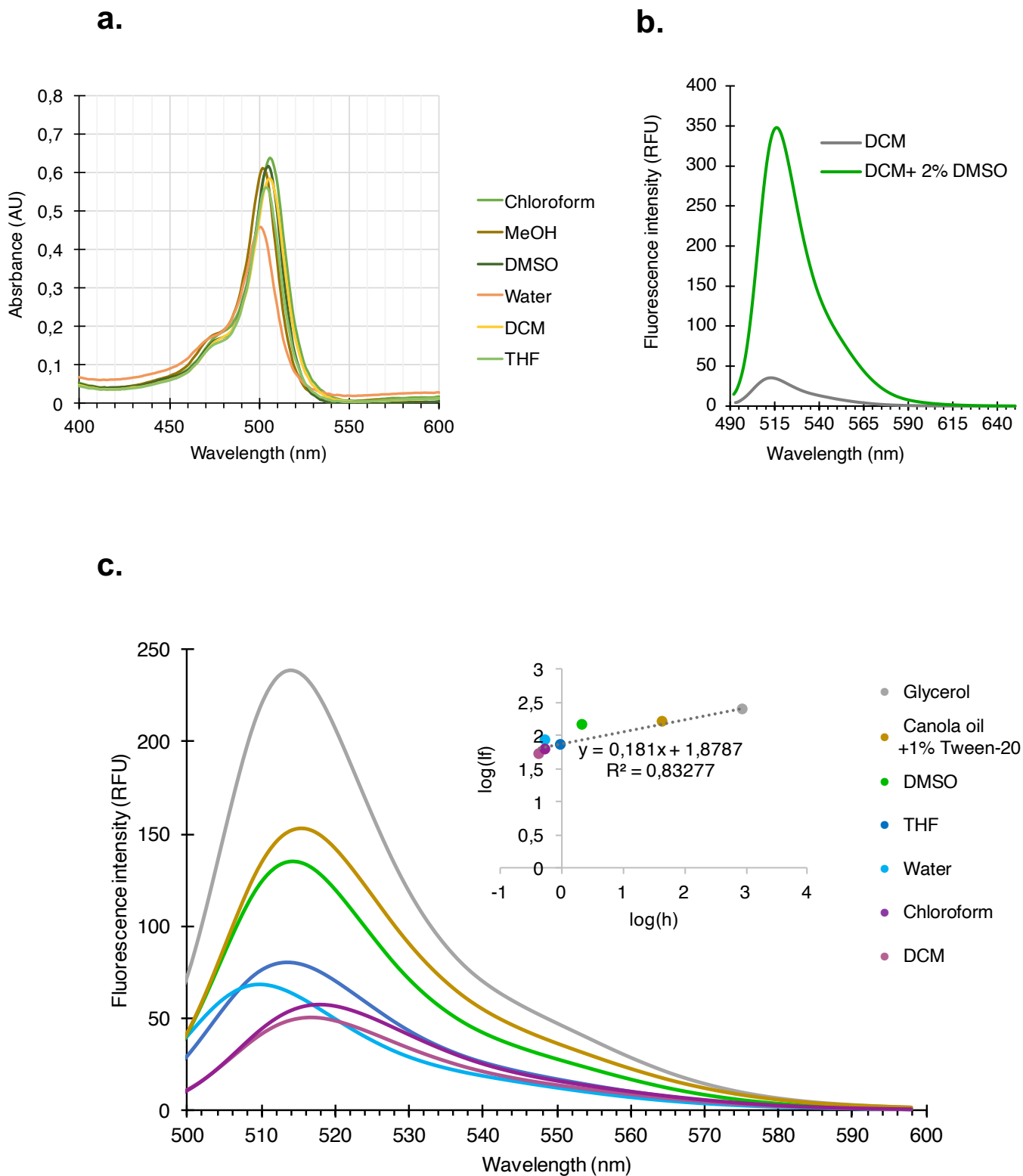


Figure S3 – Photophysical properties of **IrBDP** and **IrBDP⁺**

- a.** Electronic absorption spectra of **IrBDP⁺** (10 μ M) in various solvents containing 0.1% DMSO (v/v)
b. Fluorescence emission spectra of **IrBDP** (10 μ M in DCM) and **IrBDP⁺** (10 μ M in DCM/DMSO 98:2)
c. Fluorescence spectra of **IrBDP⁺** (10 μ M) in various solvents containing 0.1% DMSO (v/v)
 Inset: Viscosity response of **IrBDP⁺** (h: viscosity in cP)

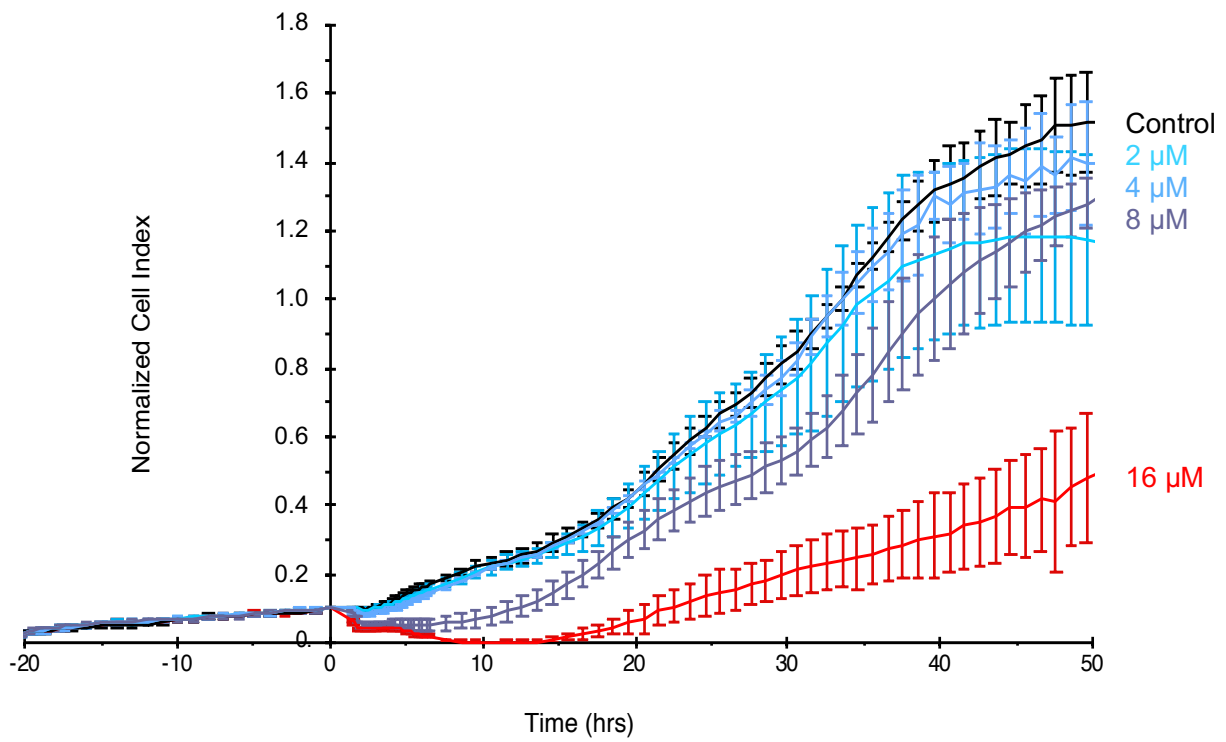


Figure S4 – Inhibition of hTERT-RPE1 cells proliferation upon IrBDP treatment
xCELLigence proliferation curves of hTERT-RPE1 cells treated with IrBDP at the indicated concentration or with vehicle (control : DMSO).

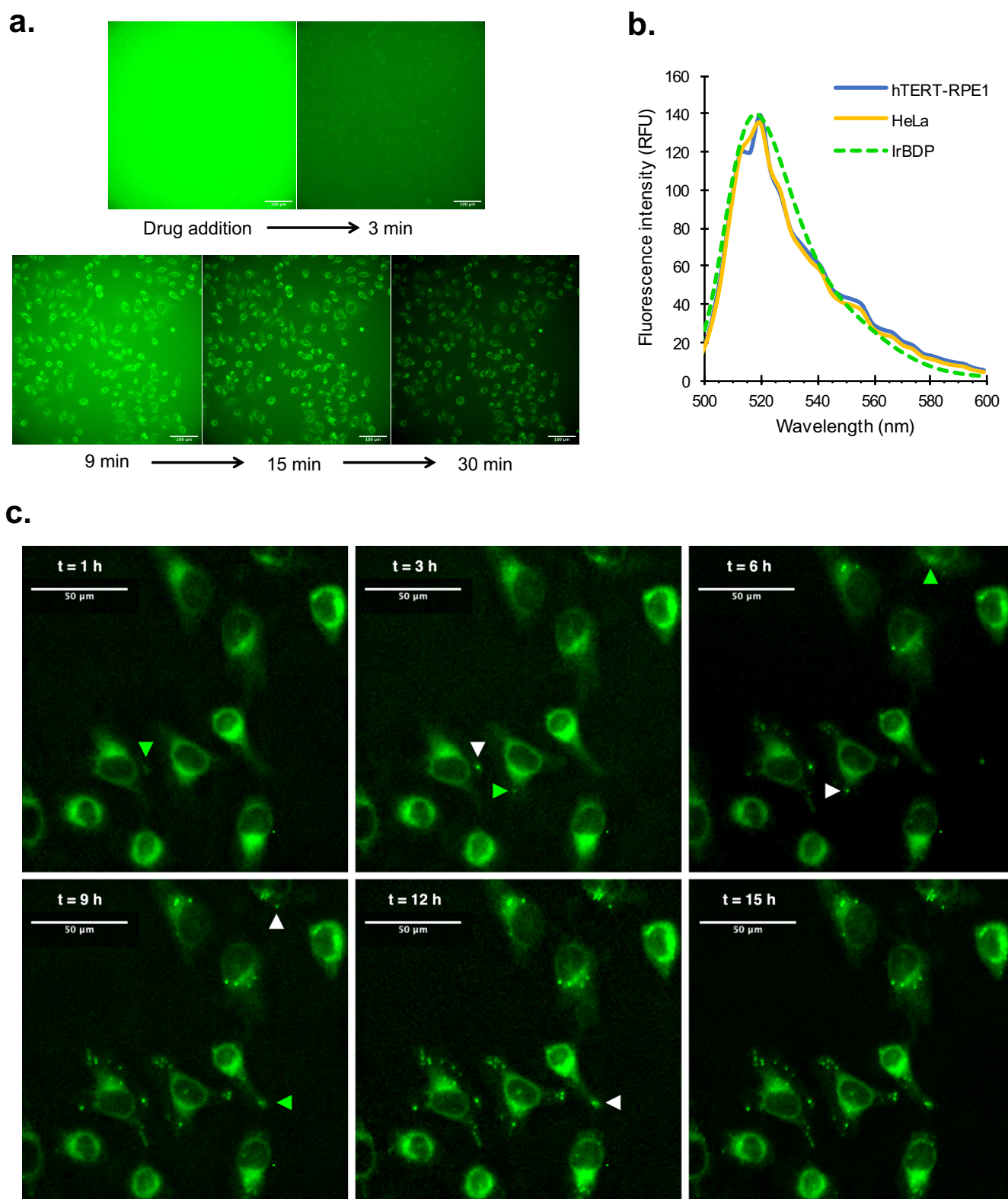


Figure S5 – Cellular uptake of IrBDP

a. Time-lapse fluorescence microscopy showing the internalization of **IrBDP** (10 μ M) in live HeLa cells over 30 min.

b. Fluorescence spectra of HeLa (orange) and hTERT-RPE1 cells (blue) treated with 8 μ M **IrBDP** for 30 min, fixed with 4% PFA (15 min) and mounted. The spectrum of **IrBDP** (in CHCl_3) is overlaid for comparison (dashed, green).

c. Time-lapse fluorescence microscopy showing live HeLa cells after treatment with **IrBDP** (10 μ M, 45 min) and two PBS washes. Snapshots from Supplementary video 4, arrows indicate nascent (green) and mature (white) punctate structures forming over the course of several hours.

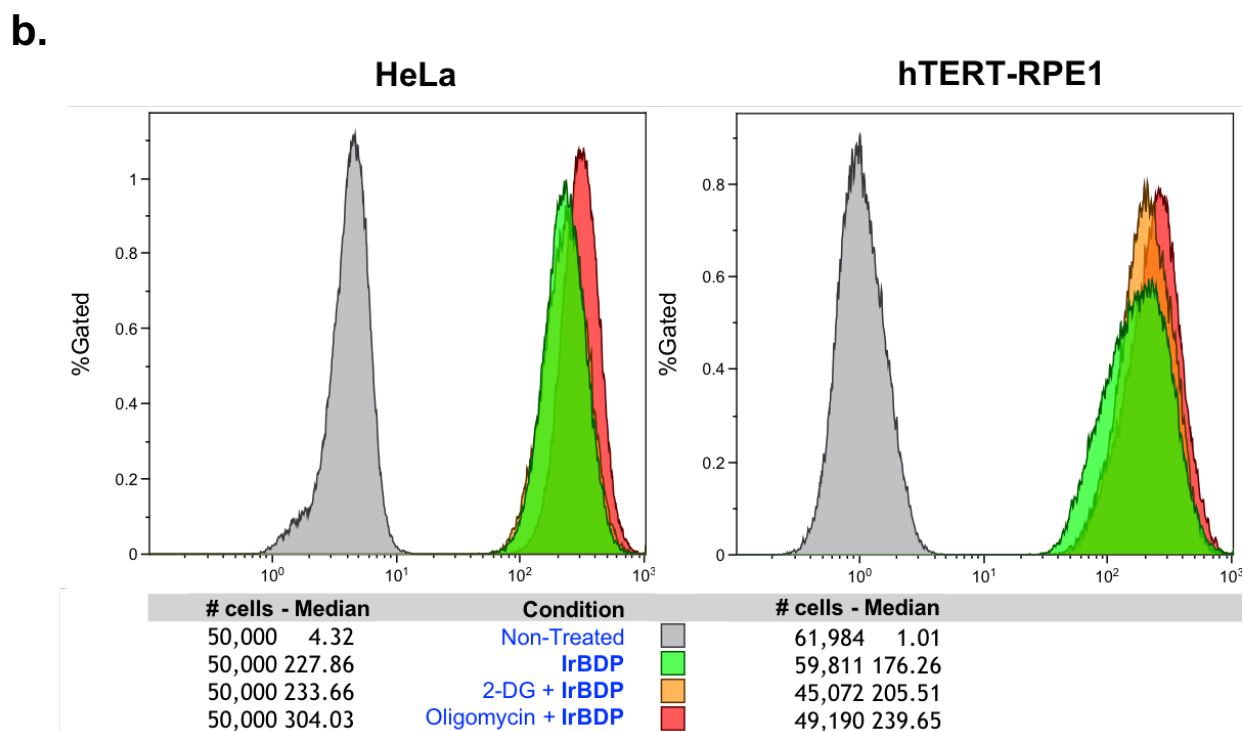
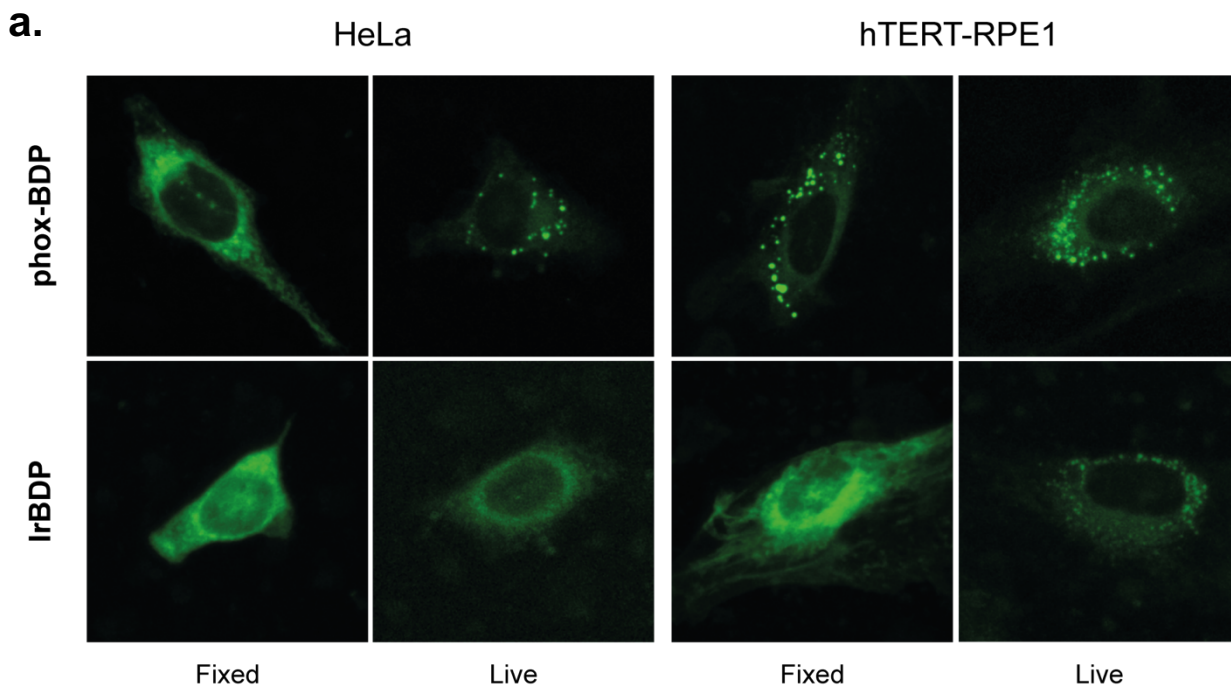


Figure S6 – Mechanism of internalization of IrBDP and phox-BDP

a. Live or fixed HeLa and hTERT-RPE1 cells stained with either IrBDP or phox-BDP (1 μ M, 30 min) and imaged by confocal microscopy (z-projections of four 210 nm confocal slices)

b. Prior to IrBDP treatment (15 min, 5 μ M), adherent cells were exposed to 50 mM 2-deoxyglucose (2-DG, glycolysis inhibitor) or 5 μ M Oligomycin (inhibitor of the respiratory chain) for 30 min to prevent ATP production and block subsequent energy-dependent internalization processes. Cells were detached with 0.05% Trypsin-EDTA, fixed with 4% PFA (15 min) and cell fluorescence (ex 488 nm, em 505-545 nm) was analyzed with a Gallios (Beckman Coulter) flow cytometer.

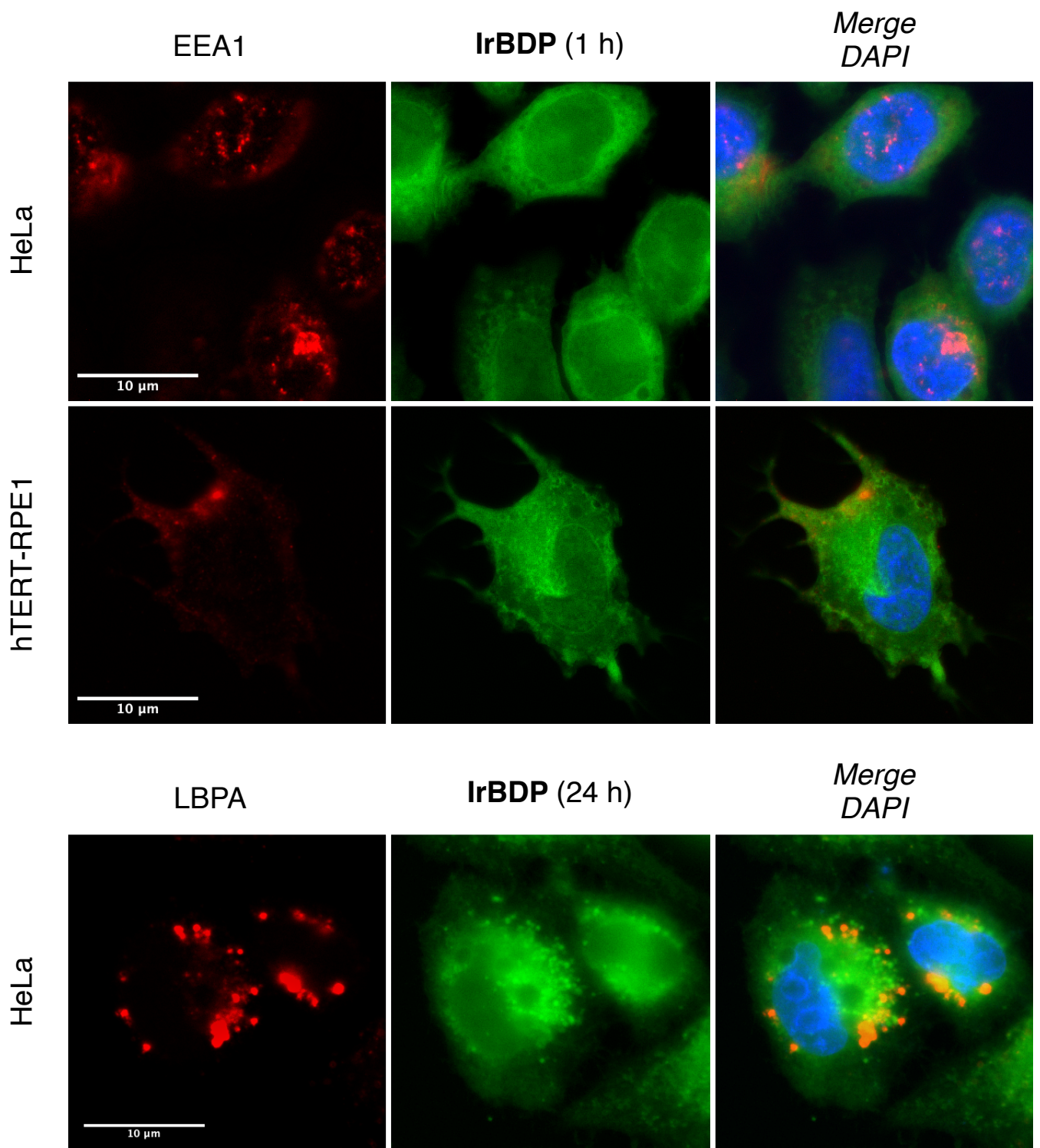


Figure S7 – **IrBDP** is not internalized by endocytosis
 Immunofluorescence of vesicles positive for EEA1 or LBPA (early and late endosomes) and comparison with **IrBDP** staining. No colocalization is observed with EEA1 after 1 h of treatment nor LBPA after 24 h, as seen by epifluorescence microscopy. Nuclei were stained with DAPI.

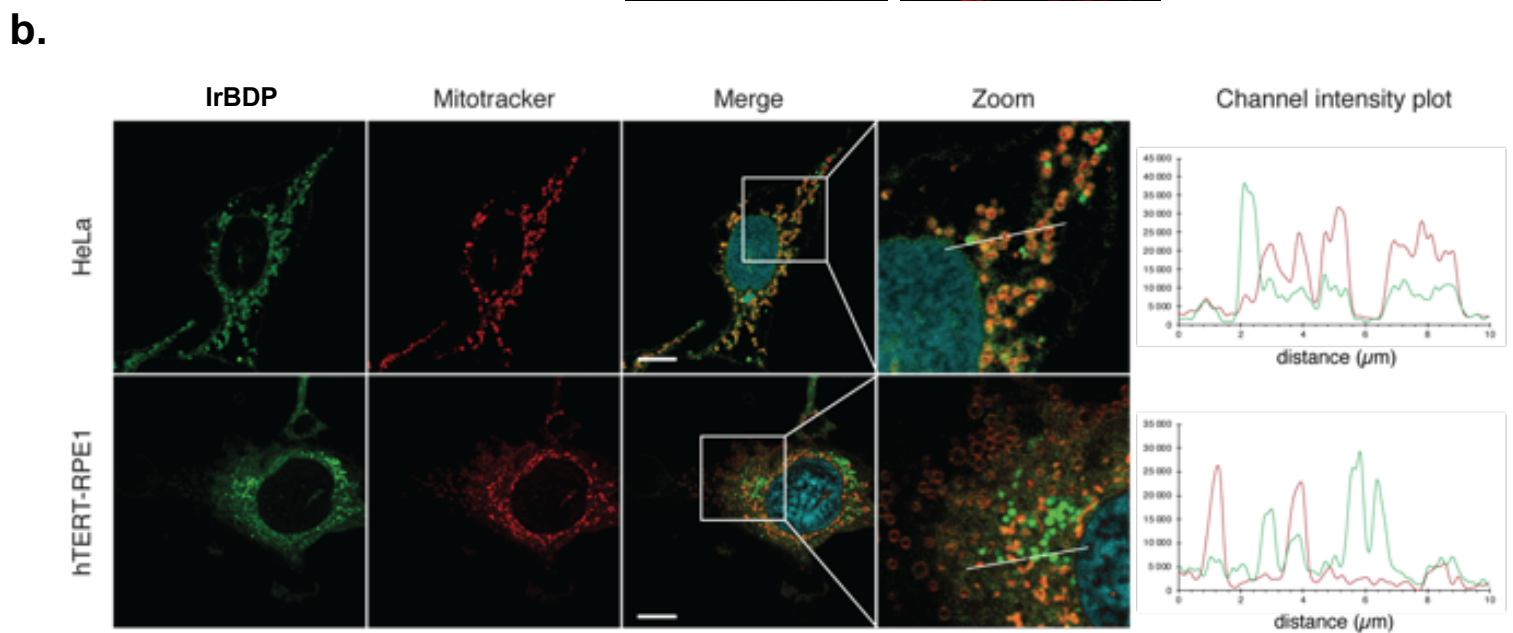
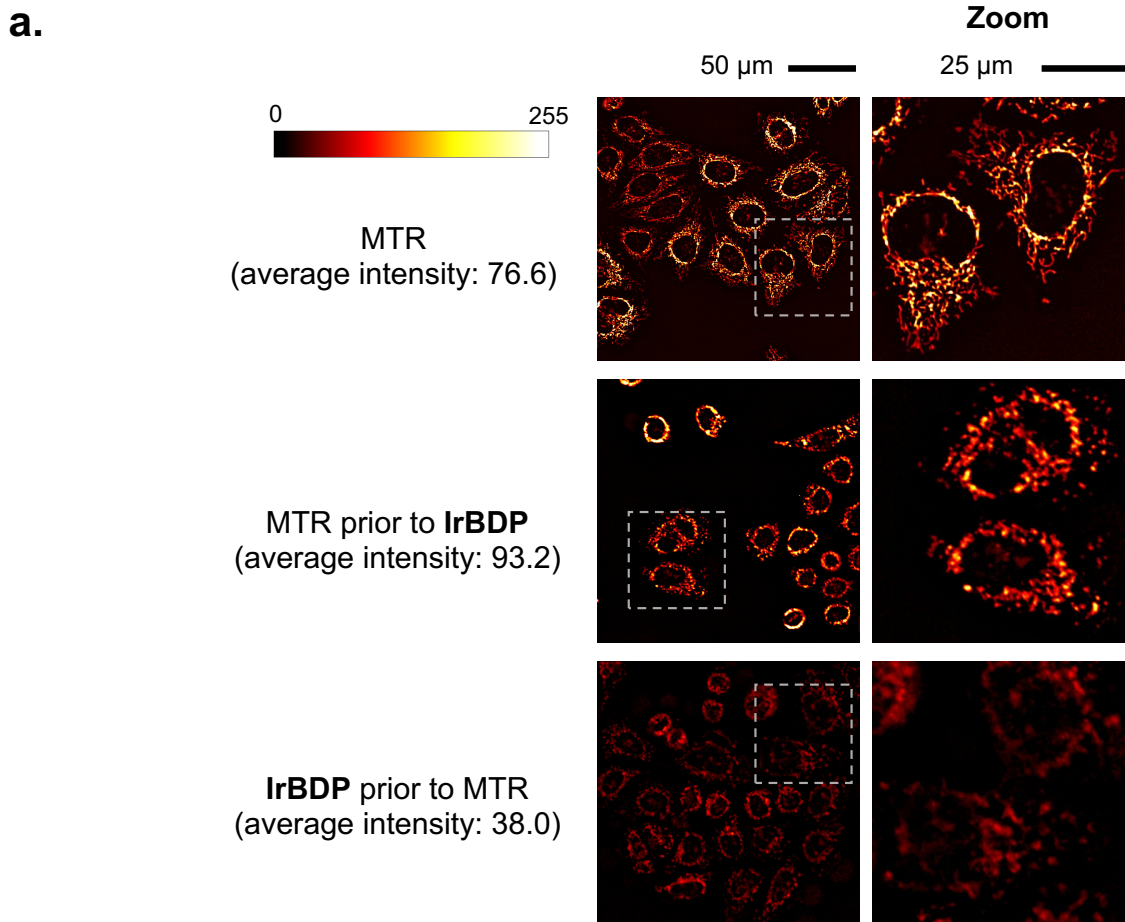
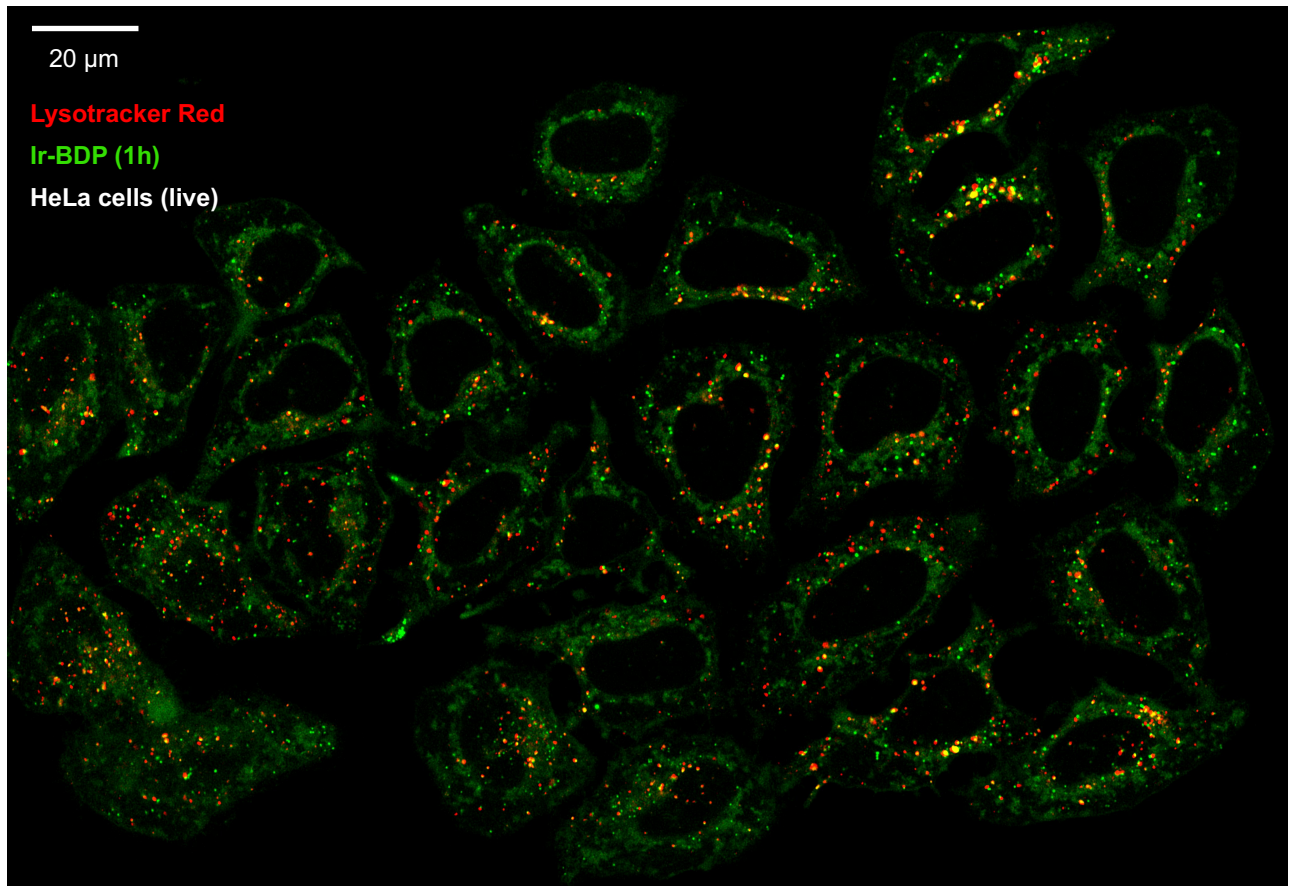


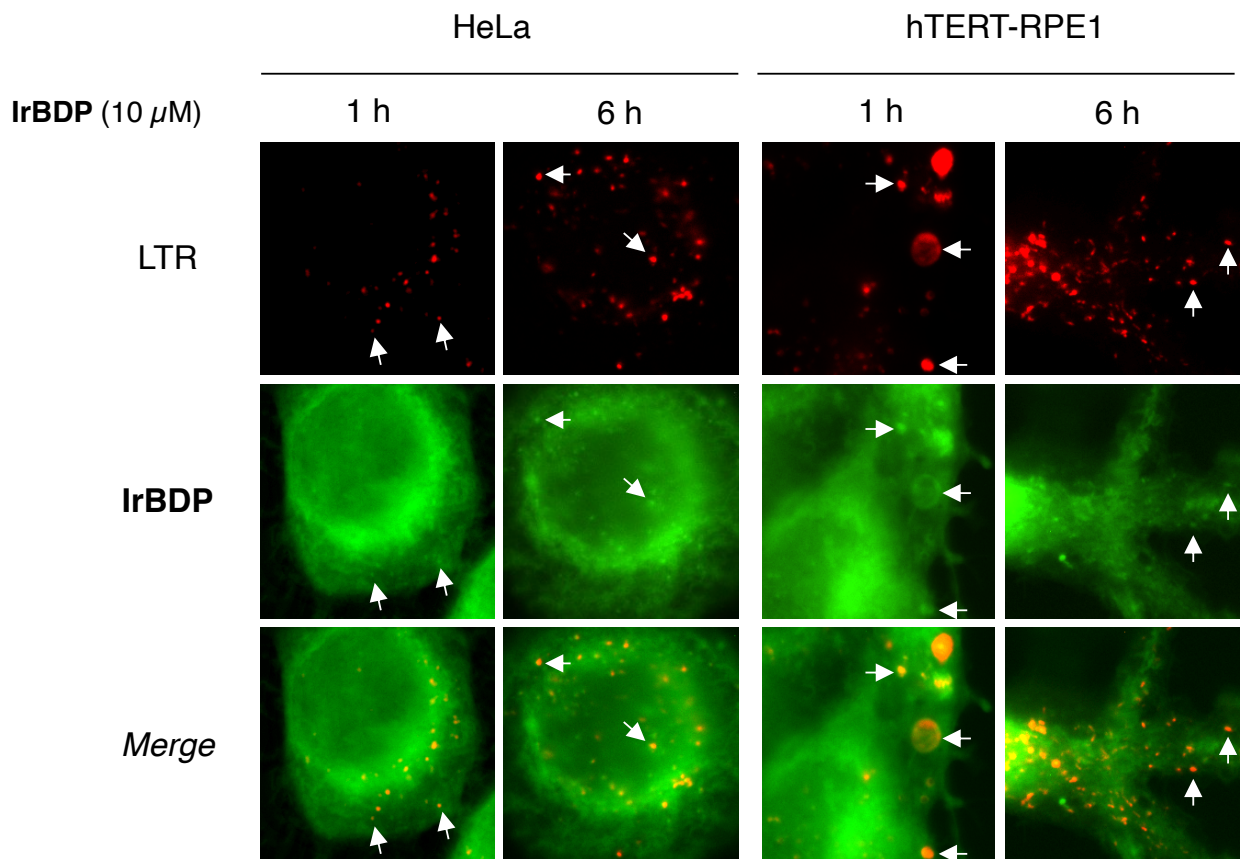
Figure S8 – IrBDP accumulates in the mitochondria

- a.** Administration of IrBDP prior to MTR prevents mitochondria labelling (false-color).
b. Co-staining of live HeLa and hTERT-RPE1 cells with MTR (red), IrBDP (green) and DRAQ5 (cyan).

a.



b.



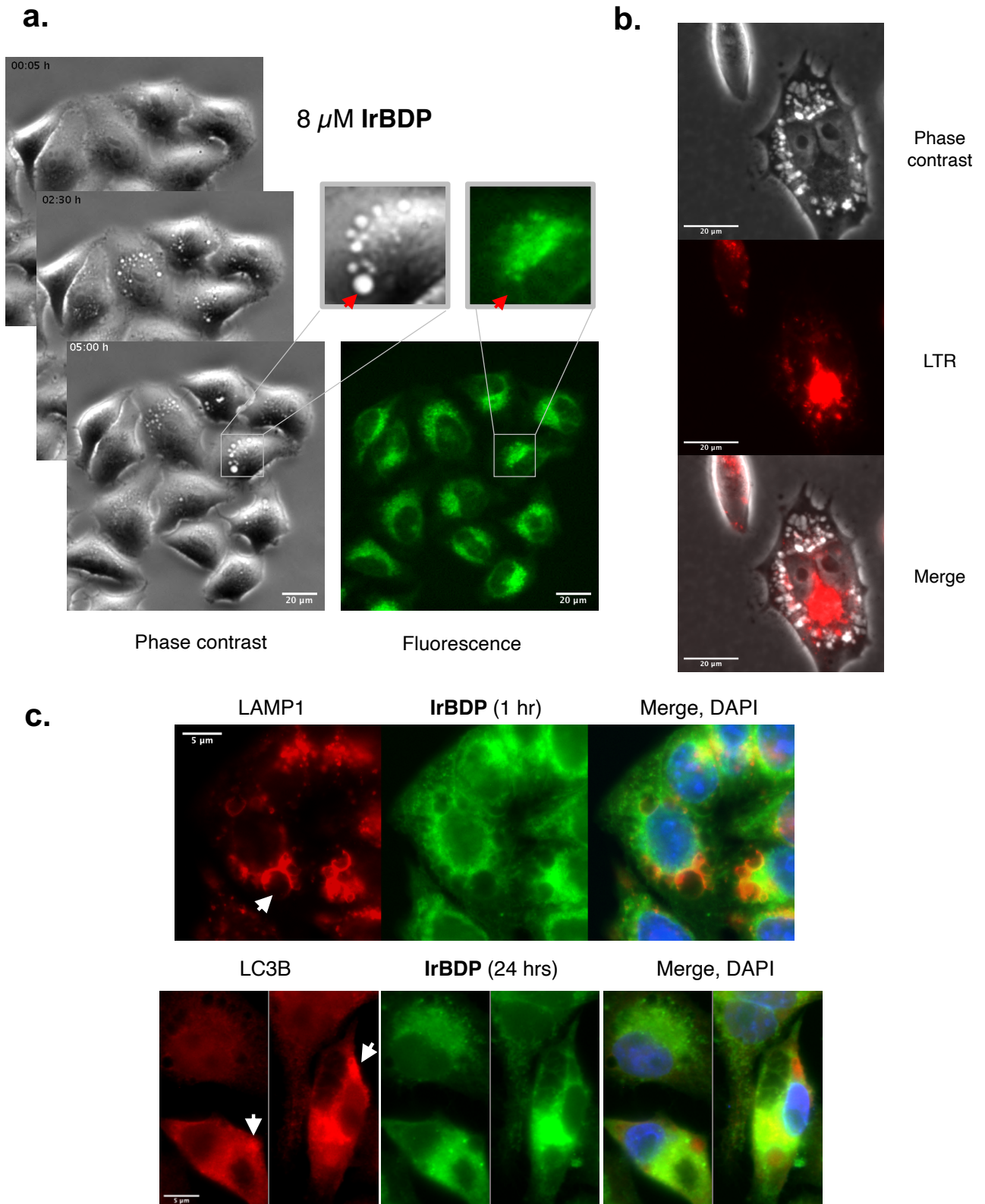


Figure S10 – Characterization of cytoplasmic vacuoles formed upon **IrBDP** treatment

a. Differential phase contrast microscopy of HeLa cells at the indicated time after addition of **IrBDP**. Cells display large refringent vesicles that increase in size and merge over time. These vesicles are **IrBDP**-negative.

b. Live-staining with LTR of a cell displaying the same phenotype of cytoplasmic vacuolization. The vacuoles are not LTR-positive and therefore non-acidic.

c. LAMP1 immunofluorescence of cells exposed to 100 nM Bafilomycin for 4h30 and 8 μ M **IrBDP** for the last 3h30. LC3B immunofluorescence of cells exposed to 10 μ M **IrBDP** for 24 h and 100 nM Bafilomycin for the last 4 h. Bafilomycin blocks the autophagic flux and freezes this transient phenotype. Arrows indicate positive vesicles.

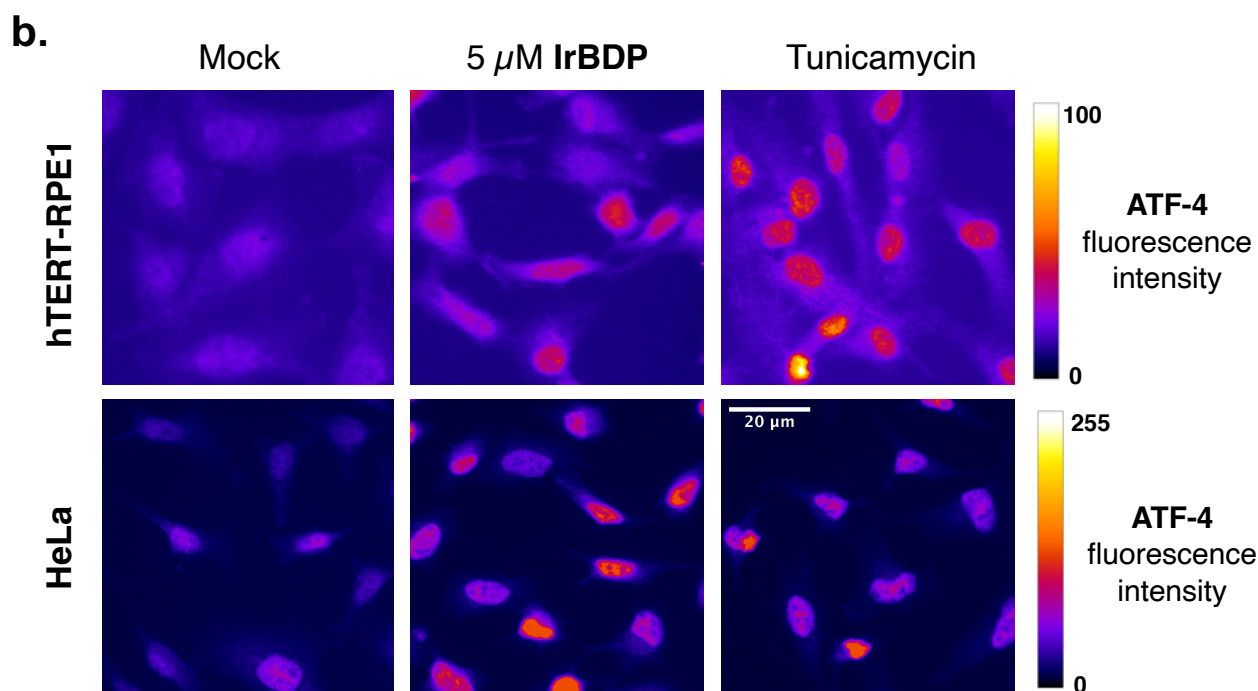
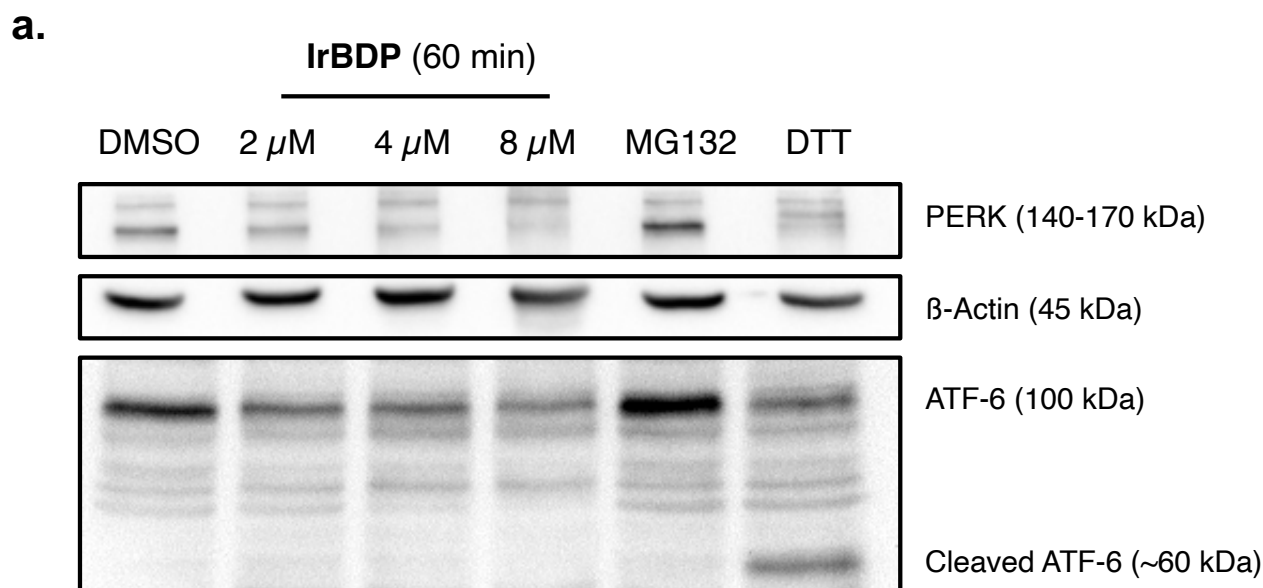


Figure S11 – ER-stress markers in response to **IrBDP** treatment

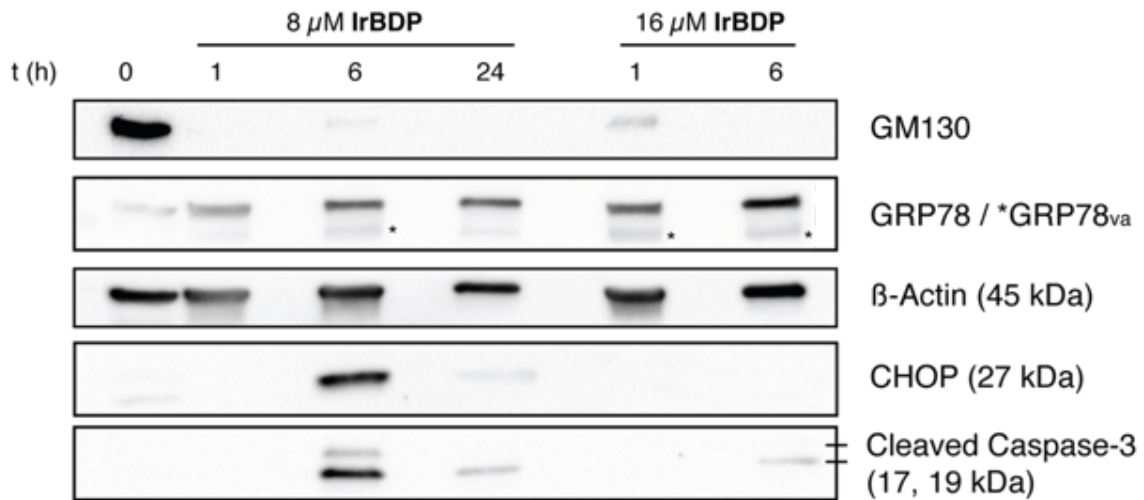
a. Cellular response to a 60 min treatment of HeLa cells with IrBDP

Western blot analysis showing the dose dependent shift of PERK and degradation of ATF-6 without production of its cleaved active form. β -Actin was used as a loading control, DTT (2.5 mM, 30 min) and MG132 (1 μ M, 60 min) were used as known ER-stress inducers. Of note, smeary bands of β -Actin were observed in **IrBDP**-treated cells (see for example 8 μ M 60 min).

b. Translocation of ATF-4 to the nucleus in response to IrBDP or Tunicamycin

Immunofluorescence analysis showing the intensity (false color) of the ATF-4 signal after treatment with either 5 μ M **IrBDP** or 1 μ g/mL Tunicamycin (positive control). HeLa cells were treated for 3 h until appearance of this signal. hTERT-RPE1 cells were treated for 6 h and 5 μ g/mL Tunicamycin. All images displayed are representative of the observed phenotype in the condition and were acquired with constant acquisition parameters for a given cell line.

a.



b.

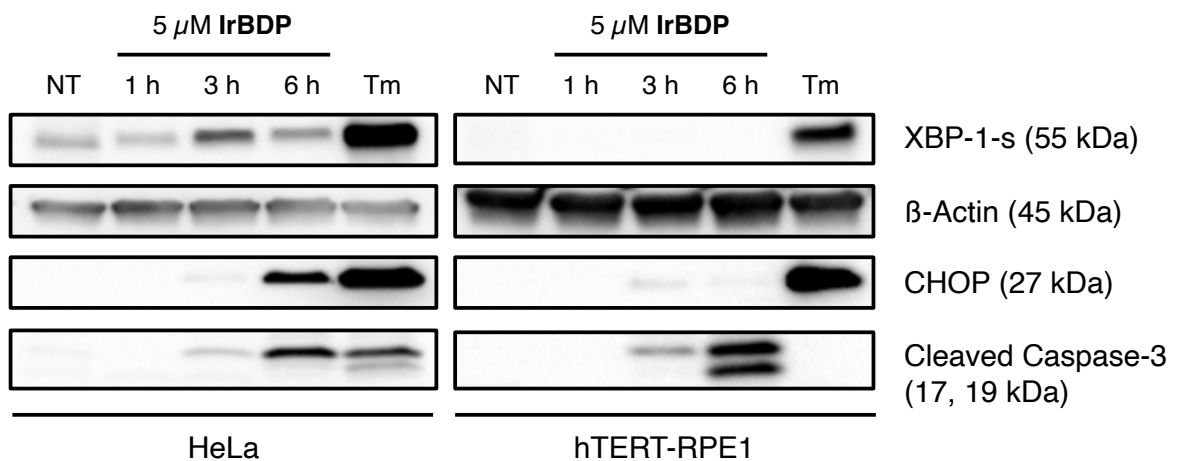


Figure S12 – Kinetics of the activation of ER-stress markers analyzed by Western Blot

a. Status of several proteins over 0 to 24 h at the indicated concentrations of **IrBDP** on the HeLa cell line. GM130 is a golgin responsible for the integrity of the Golgi apparatus. GRP78 (or BIP) is an ER abundant chaperone. *The second band was assigned to GRP78_{va}, a cytosolic variant of GRP78 expressed during ER-stress (Ni M, Zhang Y, Lee AS, *Biochem J.* **2011** doi:10.1042/BJ20101569). β-Actin was used as loading control. CHOP is a pro-apoptotic target gene of ATF-4. The presence of the cleaved form of caspase-3 illustrates apoptotic cell death.

b. Status of XBP-1-s (spliced), CHOP and cleaved caspase-3 on HeLa or hTERT-RPE1 cells exposed to 5 μM **IrBDP** at the indicated time or Tunicamycin (Tm, 1 or 5 μg/mL) for 6 h. XBP-1 is a substrate of phosphorylated IRE1, the presence of its spliced form shows activation of this pathway only in the HeLa cell line.

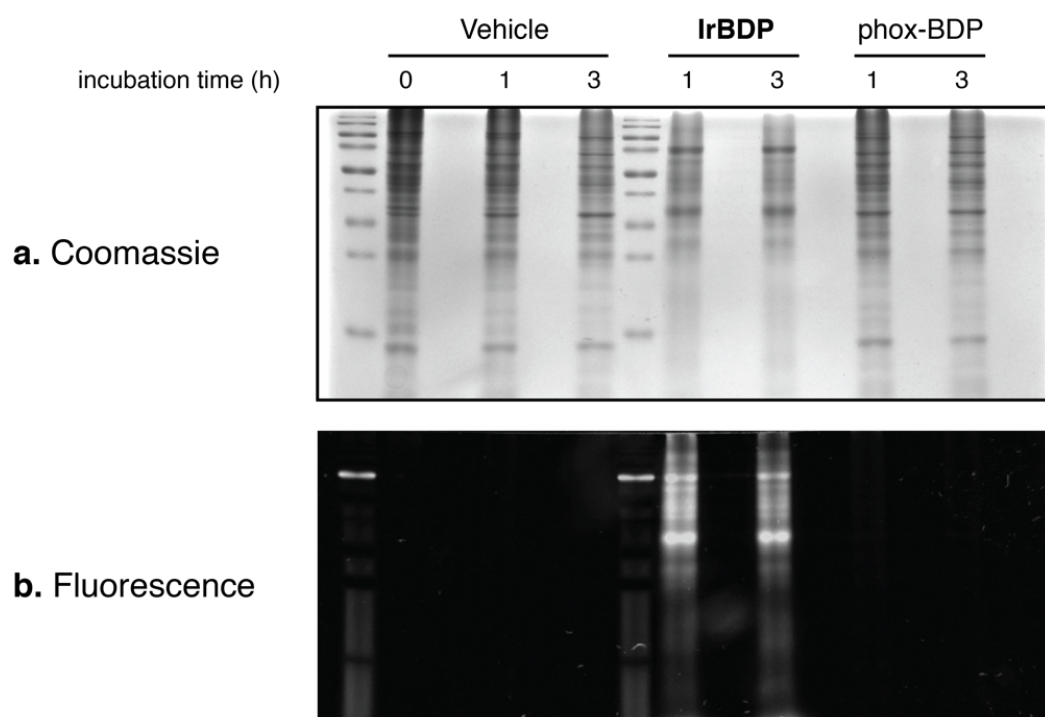


Figure S13 – **IrBDP** forms covalent adducts with proteins *in vitro*

a. Coomassie blue staining of the gel. **IrBDP** treatment induced significant changes in the profile indicating aggregation or degradation of many proteins.

b. Fluorescence acquisition (UV excitation) of the same gel before staining. The formation of fluorescent adducts is only possible with **IrBDP** but not **phox-BDP** and is time-independent.

Supplementary tables

Table S1 – Observed adducts (HRMS); relative intensity of peaks

Substrate	N-Acetyl-Cysteine Methyl ester*	N-Acetyl Histidine	Phenylbutylamine	Butyramide
Calculated m/z	897.3009	917.3349	869.3753	807.3233
Relative adduct intensity (%)	70.0	49.4	3.8	0
Observed m/z	897.3008	917.3348	869.3750	-

*adding 1 eq. NEt_3 did not change the resulting spectrum

Table S2 – Photophysical parameters of **IrBDP**, **IrBDP+** and **phox-BDP** in various solvents

IrBDP						
solvent	λ_{abs}^{max} (nm)	ϵ ($\text{l.mol}^{-1}.\text{cm}^{-1}$)	λ_{em}^{max} (nm)	Stokes' shift (cm^{-1})	Φ	τ (ns)
THF	500	53300	512	4688	Nd	Nd
CH_2Cl_2	501	53400	513	4669	Nd	Nd
IrBDP+						
MeOH	505	61100	512	2707	20.8 ± 1.4	Nd
CHCl_3	506	64000	518	4578	Nd	Nd
CH_2Cl_2	506	58300	517	4205	Nd	Nd
THF	504	56000	513	3481	Nd	Nd
DMSO	506	61700	514	3076	Nd	2.7 \pm 0.2 (70%) 3.3 \pm 0.1 (24%)
H_2O	501	45700	510	3522	Nd	2.78 \pm 0.02 (92%)
phox-BDP						
MeOH	500	41100	510	3922	25.6 ± 1.6	2.2 \pm 0.5 (87%)
DMSO	504	38400	514	3860	Nd	Nd
THF	503	36100	513	3875	Nd	Nd
H_2O	501	17800	509	3137	Nd	2.8 (74%)

Solutions of **IrBDP** and **phox-BDP** were prepared in the indicated solvents. To prepare **IrBDP+**, **IrBDP** was dissolved in DMSO and equilibrated for 24 h prior to dilution in the indicated solvents.

Nd: not determined

Supplementary videos

1- Addition of **IrBDP** in DMSO

[link](#)

2- Sample videomicroscopy: **phox-BDP** treatment

[link](#)

3- Sample videomicroscopy: **IrBDP** treatment

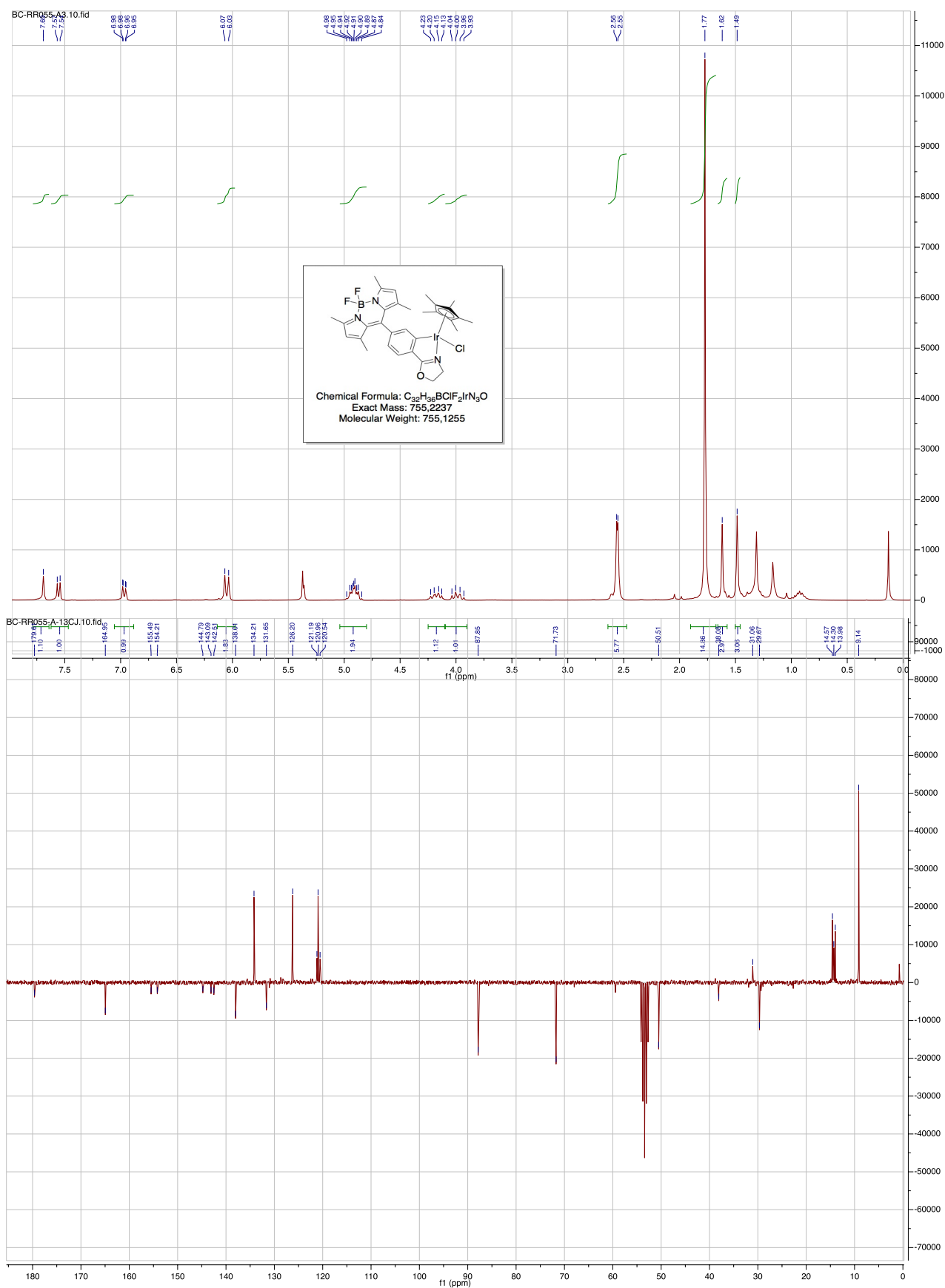
[link](#)

3- Cell fluorescence after **IrBDP** treatment

[link](#)

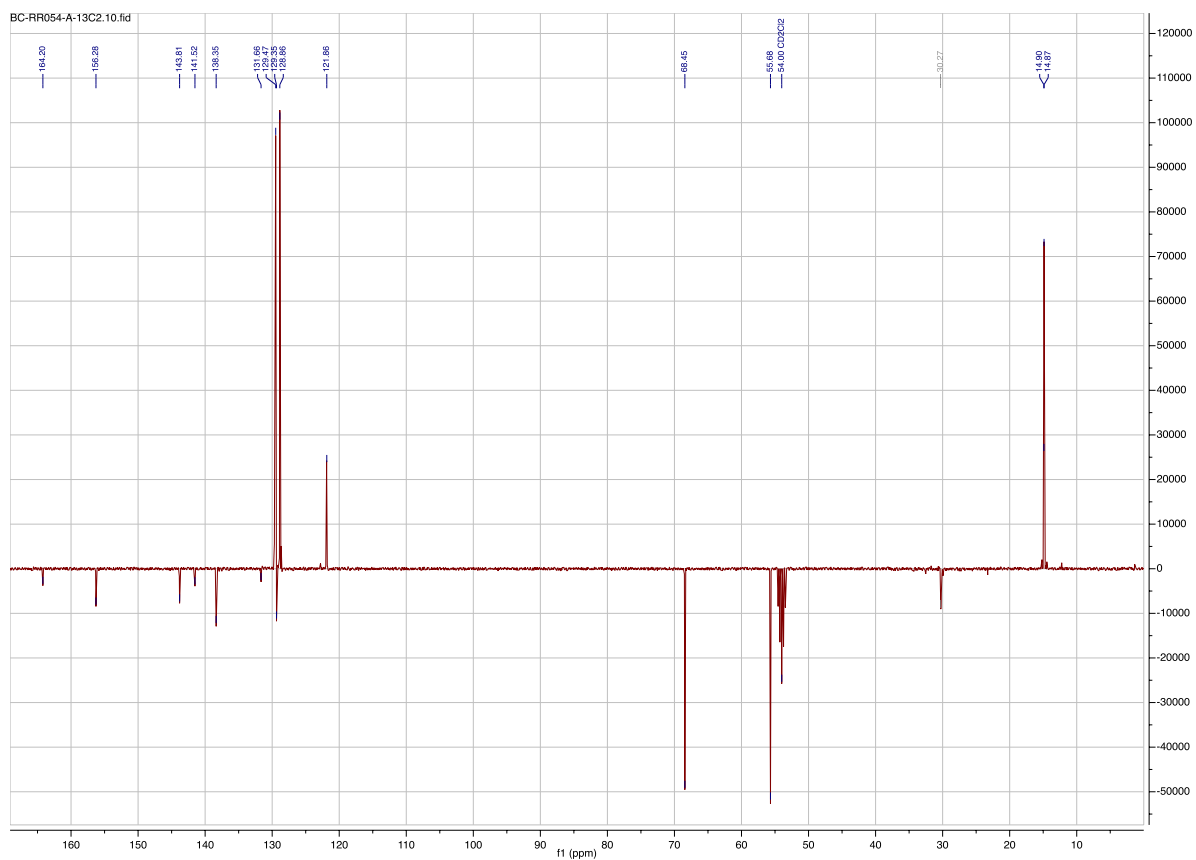
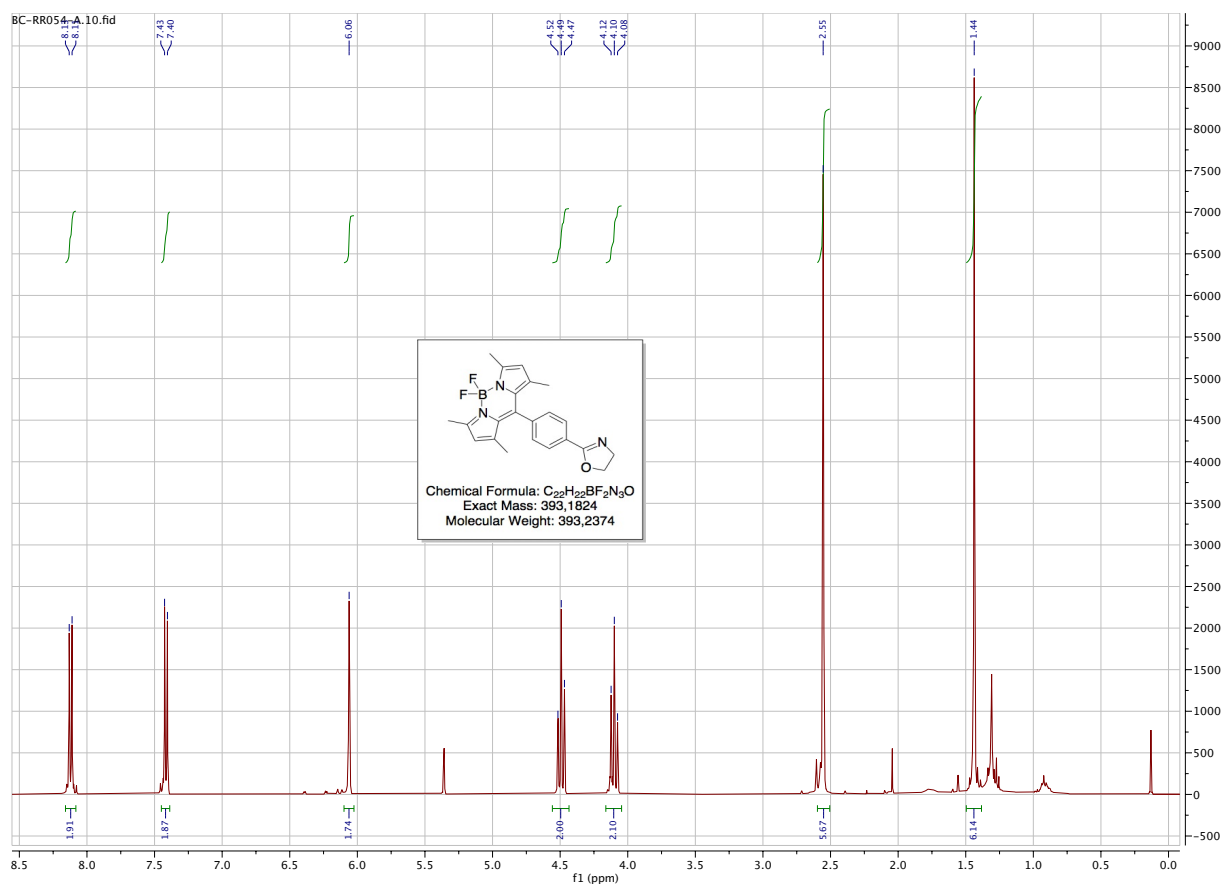
Annex 1

^1H and ^{13}C NMR spectra of IrBDP



Annex 2

^1H and ^{13}C NMR spectra of phox-BDP

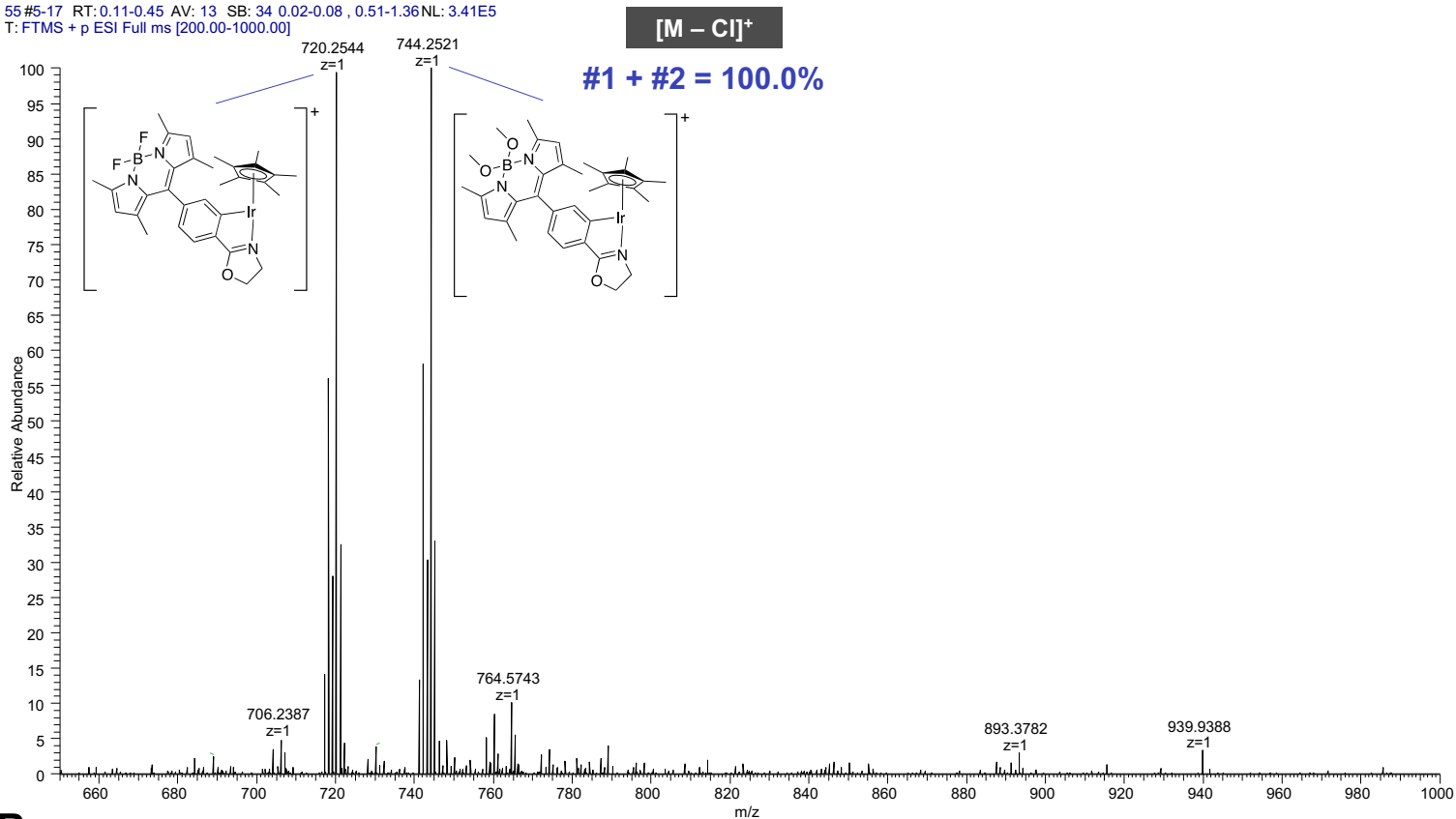


Annex 3

ESI-HRMS spectra of IrBDP alone (A) or incubated with N-AcCysOMe (B) and N-AcHis (C). (Table S1)

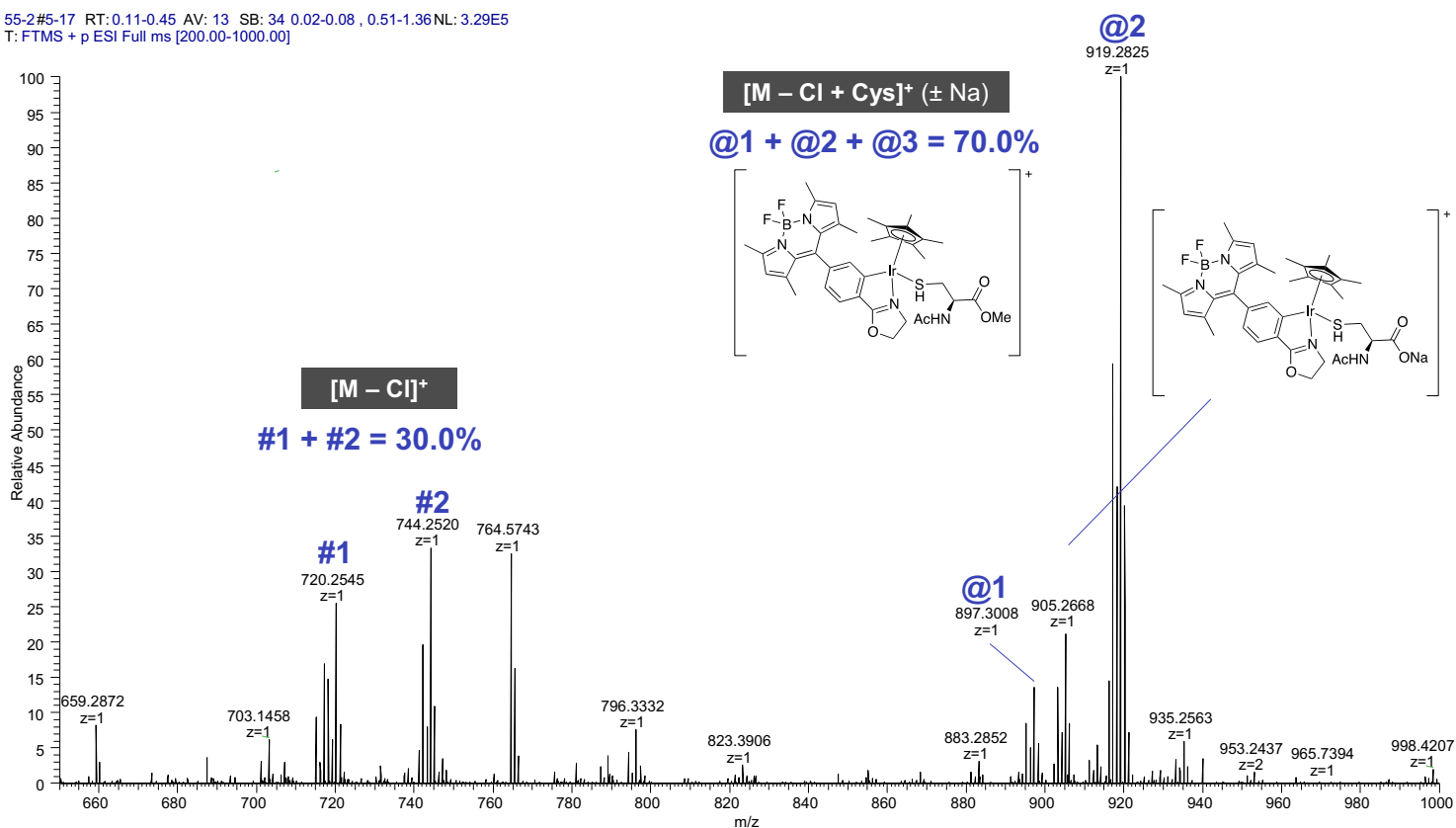
A

55-#5-17 RT: 0.11-0.45 AV: 13 SB: 34 0.02-0.08 , 0.51-1.36NL: 3.41E5
T: FTMS + p ESI Full ms [200.00-1000.00]



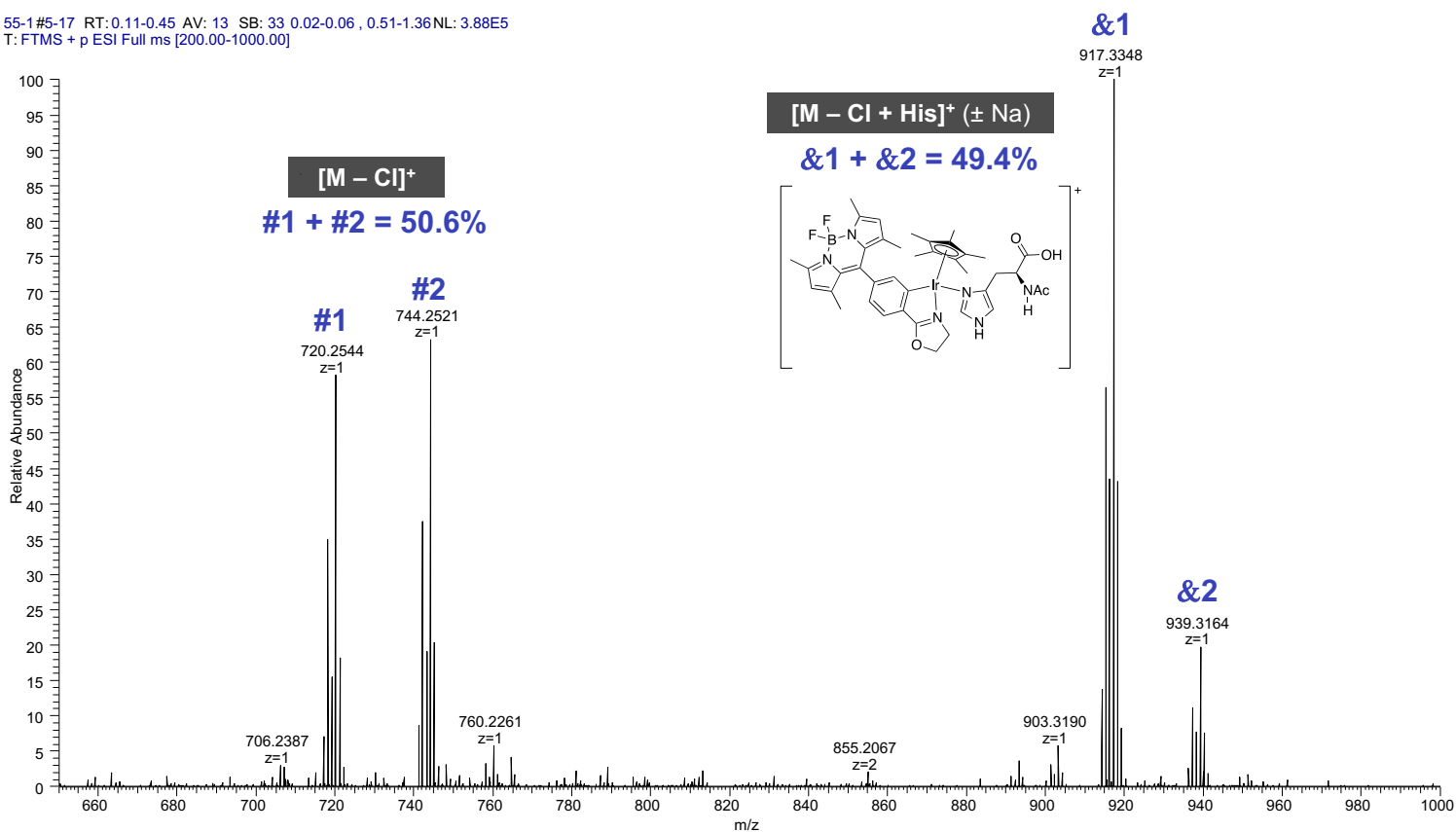
B

55-2#5-17 RT: 0.11-0.45 AV: 13 SB: 34 0.02-0.08 , 0.51-1.36NL: 3.29E5
T: FTMS + p ESI Full ms [200.00-1000.00]



C

55-1 #5-17 RT: 0.11-0.45 AV: 13 SB: 33 0.02-0.06 , 0.51-1.36 NL: 3.88E5
T: FTMS + p ESI Full ms [200.00-1000.00]



Due to relative Lewis acidity of boron atom, **IrBDP** can exchange its fluoro substituents with methanol during ionization step (presumably via HF elimination), resulting in two distinct ions separated by 23.9977 mass units (#1 to #2).

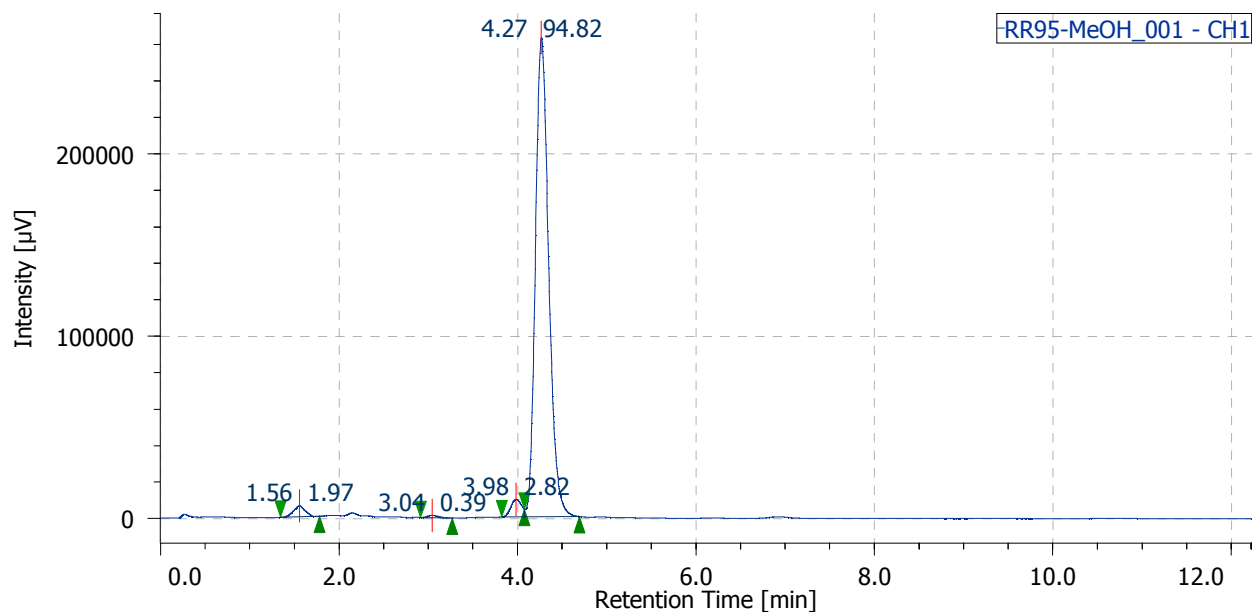
Relative intensities of total form of compounds are expressed in %. Please note that peak intensities depend on the ionizing efficiency and do not necessarily represent the amount of each species initially present in solution.

Annex 4

RP-HPLC chromatograms

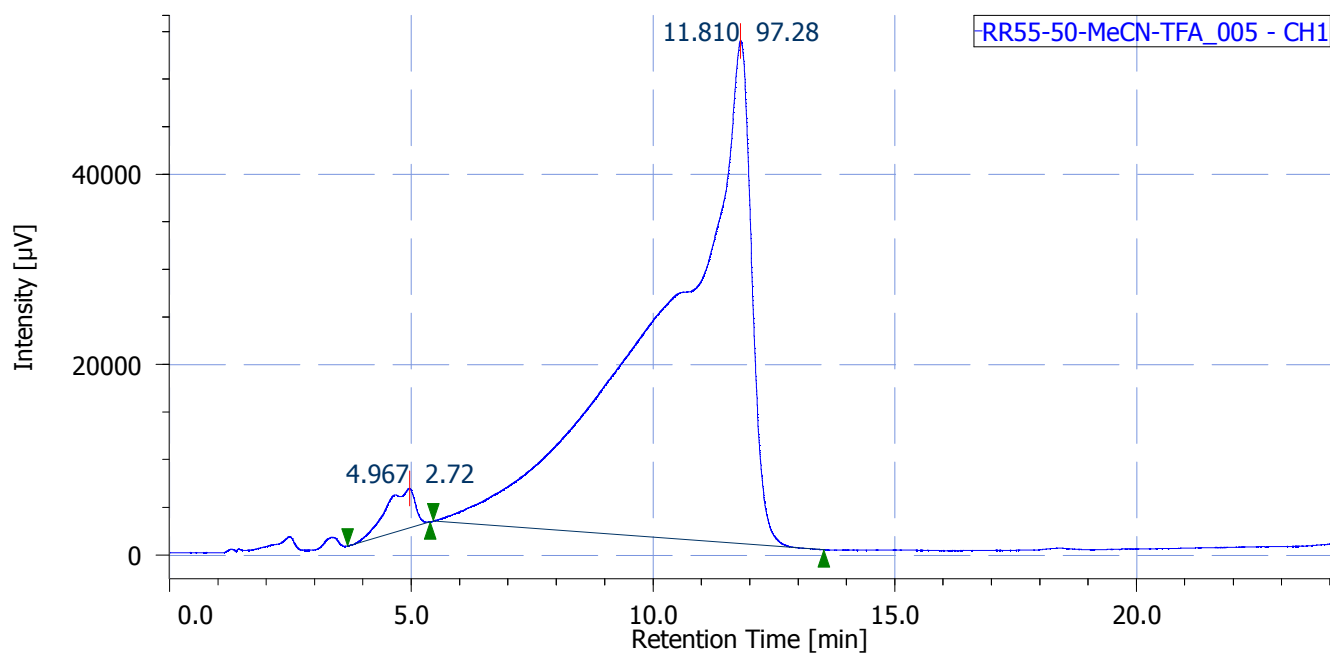
(Nucleodur C18 HTec, 150x4.6 mm, 5 µm Macherey-Nagel)

phox-BDP (100 µM, MeOH)



Eluent: H₂O / MeOH (2:8) 1 mL/min, wavelength: 254 nm

IrBDP (100 µM, MeCN 1% DMSO)



Eluent: H₂O 0.1%TFA / MeCN 0.08%TFA (1:1) 1mL/min, wavelength: 500 nm